A SINGULAR CHARACTERISTIC OF SINGLE-LAYER FREQUENCY SELECTIVE SURFACE WITH THE ELEMENT OPTIMIZED BY GA

Masataka Ohira*, Hiroyuki Deguchi, Mikio Tsuji and Hiroshi Shigesawa
Department of Electronics, Doshisha University
Kyotanabe, Kyoto 610-0321, Japan
(Tel.: +81-774-65-6371, Fax.: +81-774-65-6824, E-mail:etd1103@mail4.doshisha.ac.jp)

I. INTRODUCTION

We have developed the multiband single-layer frequency selective surfaces (FSSs) by using the optimization technique based on the genetic algorithm (GA) [1]. In the frequency responses of these FSSs for the oblique incidence, the unwanted sharp dips appear, depending on the element shape. The similar singular characteristics have been confirmed for the dipole element with the length of a wavelength [2]. But the mechanism causing such singular characteristics has not been investigated for the FSS with the complicated element shape produced by the optimization technique.

This paper makes it clear how the singular characteristics of the FSS occur in the frequency response. Firstly, we show briefly the methods for finding the singular frequency with the unwanted sharp dips, and also the resonant frequency yielding the specified reflection. Then, by using an example of the FSS developed by us, we explain the mechanism of the singular characteristics from the current distribution. Finally, the validity of the discussion is proved experimentally.

II. ANALYTICAL METHOD

The FSS is analyzed by the method of moments (MoM) [3], and then the final result can be expressed as the matrix equation $[V] = [Z][I]$. As shown in [2], the singular frequency can be obtained by solving the equation $\det[Z] = 0$ (det means the determinant of the matrix). While the resonant frequency can be obtained [4]. At the normal incidence, the imaginary part of $[V]$ becomes zero because $[V]$ means the incident wave in phase. Then, the imaginary part of the matrix equation can be approximately expressed as $[0] = [X][I]$, where $[X]$ consists of the imaginary-part elements of $[Z]$, and $[0]$ represents the zero vector. Therefore, we can obtain the resonant frequency by solving $\det[X] = 0$. It should be noted that the solutions of $\det[X] = 0$ include the singular frequencies.

III. NUMERICAL RESULTS AND EXPERIMENTS

A typical element of the GA-designed dual-resonant FSS [1] is shown in Fig. 1. By solving $\det[Z] = 0$ numerically, the singular frequencies 14.48 GHz, 24.81 GHz and 34.97 GHz can be obtained below the onset of the grating lobe at the normal incidence. The current distributions of the first two singular frequencies are shown in Fig. 1, where the vectors represent the direction and the magnitude of the current. They have the symmetric distributions and do not cause the reflection because the current vectors totally cancel each other in the element. Noting the regions divided by A-A′ and B-B′ planes shown in Fig. 1, the currents at 14.48 GHz are in phase on those planes, while those at 24.81 GHz are out of phase. So, the A-A′ and B-B′ planes can be regarded to be like the electric walls in Fig. 1(a) and the magnetic walls in Fig. 1(b). At the normal incidence corresponding to the TEM wave, the singular characteristics disappear. On the other hand, in the case of the oblique incidence, the current distribution in Fig. 1(a) is excited by TE-wave oblique incidence (E field is y polarized) rather than by TM-wave oblique incidence (E field is x polarized), and

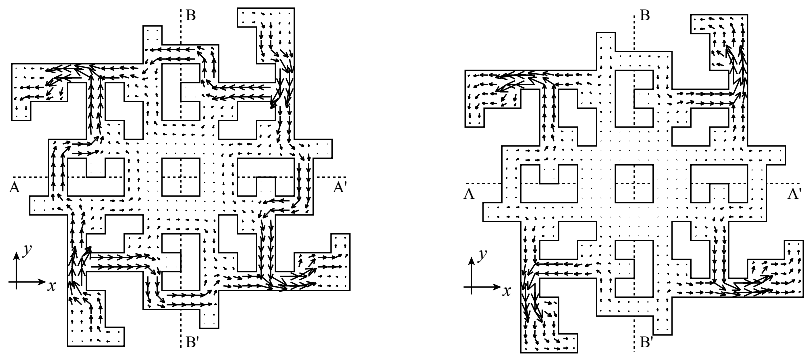

(a) 14.48 GHz. (b) 24.81 GHz.

Fig. 1. Current distributions at the singular frequencies (periodic spacing:8.0 mm).

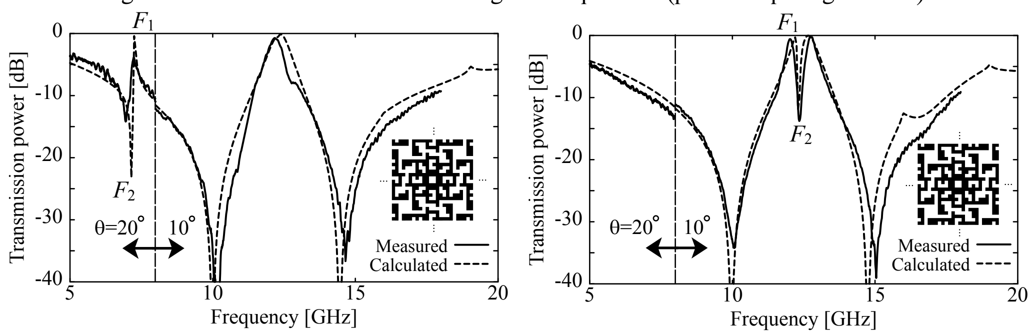

(a) TE-wave incidence. (b) TM-wave incidence.

Fig. 2. Calculated and measured transmission responses (periodic spacing:16.0 mm).

vice versa in Fig. 1(b). Next, we can approximately obtain the resonant frequencies 19.68 GHz and 28.56 GHz (excluding the singular frequencies) by solving det$[X] = 0$. We confirm that these approximate solutions are almost the same as the frequencies at the minimum transmission points obtained by solving $[V] = [Z][I]$ at the normal incidence.

Figure 2 shows the comparison of the calculated results by solving $[V] = [Z][I]$ and the measured transmission responses at the incident angles of $\theta = 10°$ and $20°$ for verifying the numerical results (the FSS is scaled up twice for the measurement). The transmissions at the frequency points F_1 are caused by the current distributions shown in Fig. 1. While the dips at frequency points F_2 are the modal interaction nulls, which can be easily understood from the equivalent circuit theory connecting the anti-resonant reactance circuit and the resonant one.

IV. CONCLUSIONS

We have discussed the singular and the resonant characteristics of the FSS with the GA-designed element shape numerically and experimentally. The understanding of these phenomena provided here will help the design of the multiband FSS.

REFERENCES

[1] M.Ohira, H.Deguchi, M.Tsuji and H.Shigesawa, "Multiband single-layer frequency selective surface optimized by genetic algorithm with geometry-refinement technique," in *IEEE Int. Symp. Antennas Propagat.*, June 2003.

[2] A. S. Barlevy and Y. Rahmat-Samii, "On the electrical and numerical properties of high Q resonances in frequency selective surface," in *Progress in Electromagnetics Research*, PIER 22, J. A. Kong, Ed., 1999, pp. 1-27.

[3] C. H. Chan and R. Mittra, "On the analysis of frequency-selective surfaces using subdomain functions," *IEEE Trans. Antennas Propagat.*, vol. AP-38, no. 1, pp. 40-50, Jan. 1990.

[4] R. F. Harrington, *Field Computation by Moment Methods*, Piscataway, NJ: IEEE Press, 1993.